Paper pa02-069
Submitted to the 28th International Conference on High Energy Physics
ICHEP'96, Warsaw, Poland, July 1996

A Determination of the Longitudinal Proton Structure Function $F_L(x, Q^2)$ at Low x at HERA

H1 Collaboration

Abstract

A precise measurement of the inclusive deep inelastic electron-proton cross section at momentum transfers $7.5 \leq Q^2 \leq 42\ GeV^2$ and large inelasticity values $0.6 \leq y \leq 0.78$ is used to determine the longitudinal proton structure function F_L at HERA for the first time. The determination of the F_2 structure function at lower y values is employed to subtract the F_2 contribution to the cross section using a NLO QCD fit to F_2 which is extrapolated into the high y region. An average value of $F_L = 0.54 \pm 0.03(stat) \pm 0.22(syst)$ is obtained for a Bjorken x range $0.00011 \leq x \leq 0.00080$, in agreement with QCD expectations based on the gluon distribution at low x.

1 Method

For about 30 years, deep inelastic lepton-hadron scattering experiments have been of fundamental importance for the investigation of proton substructure. Since the advent of the electron-proton collider HERA a new kinematic range is being explored permitting the study of the high parton density region at very low Bjorken x. Rather precise measurements of the proton structure function $F_2(x, Q^2)$ have been made at HERA [1, 2]. At lower values of the inelasticity variable $y = Q^2/sx$ this structure function dominates the inclusive scattering cross section, which in the one-photon exchange approximation is given by the expression

$$\frac{d\sigma}{dxdQ^2} = \frac{2\pi\alpha^2}{Q^4 x} \cdot [(2(1-y) + y^2)F_2(x, Q^2) - y^2 F_L(x, Q^2)] \quad (1)$$

where $s = 4E_e E_p$ is the centre of mass energy squared of the collision. This paper presents the preliminary result of a first determination of the longitudinal structure function, $F_L = F_2 - 2xF_1$ at low x at HERA. Previous fixed target experiments [3] have measured this quantity, expressed as the ratio $R = \sigma_L/\sigma_T = F_L/2xF_1$, at higher values of x.

The H1 measurement [1] of F_2 was limited to y values below 0.6 and assumed a QCD calculation of F_L. At large y, however, the weights of F_2 and F_L in eq.(1) become of comparable size. The H1 collaboration has thus attempted to reverse that procedure, i.e. to measure the cross section at the maximum possible y and derive now F_L assuming that F_2 is given by QCD. At HERA the measured y extends over about two orders of magnitude and F_2, combined with the high x data from muon scattering experiments, is well described by standard perturbative QCD with a high level of accuracy. Thus the contribution to the cross section of F_2 can be reliably determined from a NLO QCD fit to F_2 and subtracted from the measured cross section. The basic, unavoidable assumption of this procedure, until one has data at different HERA beam energies, remains that F_2 can indeed be extrapolated using QCD into the high y region, i.e. from lower to larger Q^2 at fixed x. This appears to be reasonable, given the impressive agreement of the F_2 measurements over 4 orders of magnitude in Q^2 with DGLAP QCD evolution, yet it is not true necessarily as this measurement covers the lowest accessible x values at a given Q^2. An advantage of the method is due to the fact that the F_2 and the F_L measurements are performed using the same data, though in different regions of y, which leads to partial cancellations of systematic errors.

2 Measurement

The data were taken in 1994 with positrons of $E_e = 27.5\ GeV$ and protons of $E_p = 820\ GeV$. The analysis is based on the "nominal vertex data" [1] for $Q^2 \geq 7.5\ GeV^2$ which enabled the most precise inclusive cross section measurement of H1 so far. This and the trigger, event selection and analysis are described in detail in the recent F_2 publication [1].

The kinematic variables were reconstructed using the scattered electron angle θ_e and energy E'_e which were measured in the backward proportional chamber (BPC), combined with the event vertex, and the backward electromagnetic calorimeter (BEMC).

The necessity of extending the y range of the measurement by lowering the scattered positron energy from 11 GeV to 6.5 GeV introduced the following peculiarities of the F_L analysis over the standard one: i) data were included using a lower threshold BEMC trigger in coincidence with a central proportional chamber trigger; ii) in the extended kinematic range $0.6 \leq y \leq 0.78$ and $7.5\ GeV^2 \leq Q^2 \leq 42\ GeV^2$ it was possible to require a signal in the inner central proportional chamber which has been important to reduce background due to neutral particles from photoproduction; iii) more than one charged track was required in the central drift chamber (CJC) which corresponded to the additional track trigger requirement.

The BEMC trigger was monitored with a CJC trigger and found to be efficient to better than 98%. The proportional chamber trigger was monitored with another BEMC trigger and found to be efficient to better than 96%. In order to monitor this BEMC trigger at the lowest energies, from 6.5 to 8 GeV, a model of the trigger response had to be built which described its efficiency very accurately as functions of the hadron and electron angles and of the track multiplicity.

The selection of electrons was studied based on the Monte Carlo simulated events and also by detailed investigation of the experimental first and second energy cluster distributions which were found to be very well reproduced by the simulation in shape and absolute normalization. The photoproduction background was monitored using the electron tagged photoproduction events, the inner proportional chamber and studying those events which were rejected by the electron identification cuts. The relative amount of photoproduction events depends on Q^2. On average it is 16% with an estimated error of 3%.

Fig.1 displays the distributions of the BEMC energy for the DIS events and for the background events. The shape is well described by the simulated spectra which are normalized to the luminosity $(1.25 \pm 0.17)\ pb^{-1}$ of the data which comprise about 70% of the statistics of the F_2 analysis [1] because of a very strict data selection and due to prescaling of the main trigger used here. The analysis lead to another, independent measurement of the F_2 structure function with an extension by one bin towards lowest x in the considered Q^2 range. This is illustrated in fig.2 showing the published data together with this analysis for $Q^2 = 25\ GeV^2$. Both analyses agree very well. To illustrate the sensitivity to F_L two dashed lines are drawn, the upper line representing F_2 as it would have been obtained assuming $F_L = 0$ and the lower line for $F_L = F_2$. These two limits correspond to a ratio of $R = F_L/(F_2 - F_L)$ equal to zero or infinity, respectively.

3 Result

The cross section measurement was converted to a determination of F_L by subtracting the contribution of F_2. The latter is determined using the result of a NLO DGLAP QCD fit [1] to F_2 which was performed for $y < 0.35$ where the sensitivity to F_L is reduced, and is shown as the solid curve in Fig.2. The radiative corrections were studied extensively. For example, by imposing the cut $y \geq 0.1$, with y reconstructed from the hadronic final state, a large part of the corrections is suppressed but the final result appears to be stable within about half of the statistical errors. Based on the HECTOR code [4] the corrections were subtracted absolutely from the cross section and were not applied multiplicatively in order to reduce their dependence on F_L. A bin center correction was applied. The resulting F_L points in six bins of Q^2, or equivalently of x, are shown in Fig.3. The systematic errors are highly correlated from point to point and are very similar for all F_L values because they mainly depend on y. Thus the systematic error is drawn in Fig.3 as one error band of the width ± 0.22 around the central average F_L value which was obtained assuming F_L to be independent of x or Q^2 at constant y.

There are three main systematic error contributions which were carefully disentangled and studied:

- errors which affect only the high y cross section measurement, dominated by various cut efficiency errors and, at the lowest Q^2, by the photoproduction background uncertainty. These experimental errors amount to an absolute F_L error of about 0.16;

- those errors which are common to the cross section measurements at low and at high y, like the luminosity uncertainty. In the subtraction the effect of these errors is reduced to an F_L uncertainty of 0.03;

- errors of the subtracted F_2 contribution which arise from the experimental errors specific to the lower y region, like the ones of the Σ method [1], and from the dependence on the fit assumptions like parametrizations and charm treatment, for example. These errors were estimated to be about 0.14 including the residual dependence of the lower y F_2 data on F_L.

Fig.3 shows the extreme limits of $F_L = 0$ and $F_L = F_2$ using the QCD fit. On average the measured F_L value is 2.6 standard deviations larger than zero and 4 to 5 standard deviations away from F_2. At low x the F_L structure function is related to the gluon distribution [5]. The full line in Fig.3 represents the calculation of F_L according to the QCD relation as given in [6] using the gluon (and quark) distributions determined by the QCD fit. There is consistency between the F_L and the gluon distribution determined from the scaling violations measured with F_2 in the low y range. Higher order QCD corrections are being evaluated. In the range covered an approximately constant value of $F_L \simeq 0.4$ [6] and a value of $R \simeq 0.5$ [7] were expected in earlier QCD calculations which is consistent with the result obtained.

Acknowledgments

We are grateful to the HERA machine group whose outstanding efforts have made and continue to make this experiment possible. We thank the engineers and technicians for their work in constructing and now maintaining the H1 detector, our funding agencies for financial support, the DESY technical staff for continual assistance, and the DESY directorate for the hospitality which they extend to the non–DESY members of the collaboration.

References

[1] H1 Collaboration, S. Aid et al., Nucl. Phys. **B470** (1996) 3

[2] ZEUS Collaboration, M. Derrick et al., Z.Phys. **C69** (1996) 607

[3] L.W. Whitlow et al., Phys. Lett. **B250** (1990) 193 and references to the SLAC experiments cited therein;
CCFR Collaboration, U.K. Yang et al., J. Phys. G: Nucl. Part. Phys. **22** (1996) 77;
NMC Collaboration, A. Milsztaijn, Proc.Int.Conf. on Deep Inelastic Scattering, Rome 1996, to appear

[4] A. Arbuzov et al., Comp. Phys. Comm. **94** (1996) 128

[5] G. Altarelli and G. Martinelli, Phys. Lett. **B76** (1978) 89

[6] M. Glück, E. Reya and A. Vogt, Z. Phys. **67** (1995) 433

[7] A.González-Arroyo, C.López and F.L.Ynduráin, Phys. Lett. **B98** (1981) 215

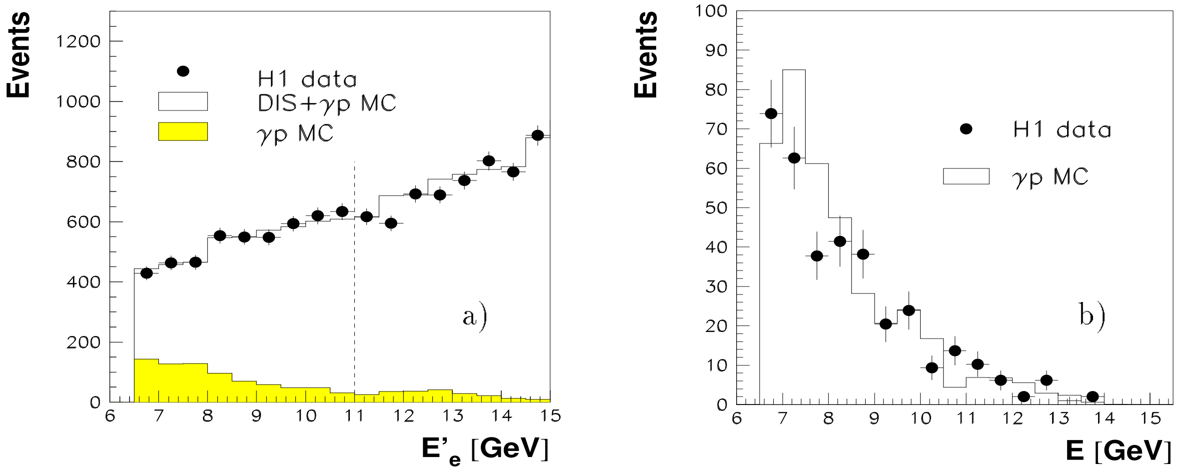

Figure 1: BEMC energy distribution at high y, a) for the selected DIS events and b) for the tagged photoproduction events. The simulated spectra, both for DIS and γp events, are normalized in absolute to luminosity.

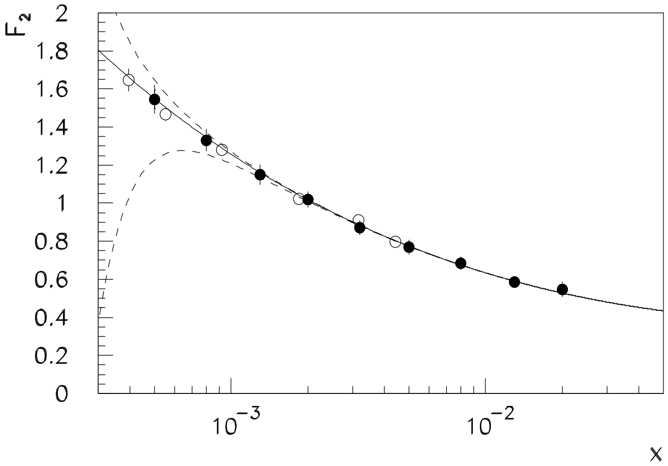

Figure 2: Comparison of this analysis (open points) and the published F_2 structure function analysis (closed points), with statistical errors for $Q^2 = 25\ GeV^2$. The full curve is a DGLAP NLO QCD fit to F_2 for $y \leq 0.35$. The dashed curves indicate the resulting F_2 if the cross section would have been evaluated assuming $F_L = 0$, upper curve, or $F_L = F_2$, lower curve.

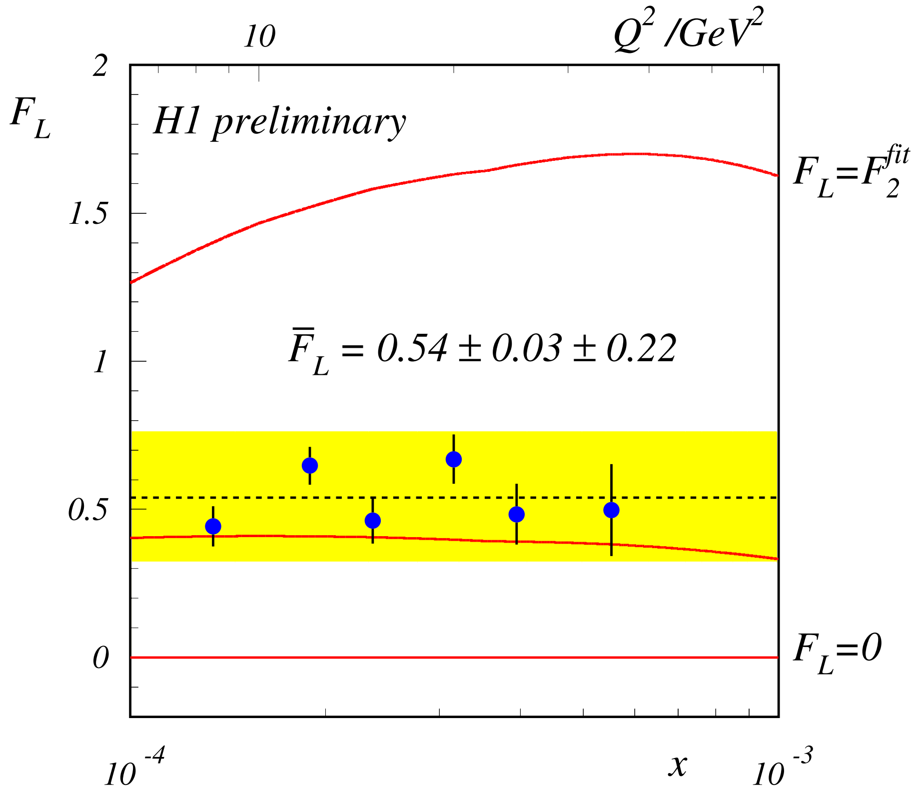

Figure 3: Measured longitudinal structure function F_L for $y = 0.7$ as functions of x and of $Q^2 = sxy$ for $Q^2 = 8.5,\ 12,\ 15,\ 20,\ 25,\ 35\ GeV^2$. The error bars are the statistical error, the band is the systematic error common to all points. The lines $F_L = 0$ and $F_L = F_2$ represent the possible limits of F_L derived from the positivity of the cross sections of longitudinally and transversally polarized photons. The solid curve is a QCD calculation of F_L based on the F_2 data measured at lower y.